

Intrinsic tunneling spectroscopy of $\text{Bi}_2\text{Sr}_2\text{CaCu}_2\text{O}_{8+\delta}$: The junction-size dependence of self-heating

X. B. Zhu, Y. F. Wei, S. P. Zhao,* and G. H. Chen

Beijing National Laboratory for Condensed Matter Physics, Institute of Physics, Chinese Academy of Sciences, Beijing 100080, China

H. F. Yang, A. Z. Jin, and C. Z. Gu

Laboratory of Microfabrication, Institute of Physics, Chinese Academy of Sciences, Beijing 100080, China

(Received 26 January 2006; revised manuscript received 1 May 2006; published 1 June 2006)

The self-heating effect on intrinsic tunneling spectra (ITSs) is investigated using stacks of intrinsic Josephson junctions (IJJs) in near optimally doped $\text{Bi}_2\text{Sr}_2\text{CaCu}_2\text{O}_{8+\delta}$ crystals. The area of the stacks S ranges from 12 down to $0.16 \mu\text{m}^2$. For IJJs with larger S , ITSs are distorted by self-heating, but become progressively less size dependent as S decreases down to submicrometer level. Analysis based on the ballistic phonon model of Krasnov *et al.* indicates a temperature rise of ~ 5 K for the smallest junctions at the bias voltage corresponding to the conductance peak. A brief comparison between the ITSs and spectra from other techniques is presented.

DOI: [10.1103/PhysRevB.73.224501](https://doi.org/10.1103/PhysRevB.73.224501)

PACS number(s): 74.50.+r, 74.25.Jb, 74.72.Hs

I. INTRODUCTION

The intrinsic tunneling spectroscopy of bismuth cuprate superconductors has recently received considerable attention.^{1–6} This technique utilizes intrinsic Josephson junctions (IJJs),^{7,8} which are unique in probing bulk electronic properties, among other important methods such as scanning tunneling spectroscopy^{9,10} (STS) and the break-junction technique.^{11,12} However, intrinsic tunneling spectra (ITSs) can be seriously affected by self-heating,^{13–21} due to poor thermal conductivity of the cuprate materials and relatively large current densities required to reach the gap voltage. Experimentally, ITSs are usually different from those obtained in STS and break-junction experiments.

It is important to eliminate the heating in order to obtain the genuine ITS. At present, efforts devoted to such a purpose have been roughly in two directions. One is the short-pulse measurement of the current-voltage (I - V) curves,^{2,14–16} which suppresses the Joule heat in the time domain. Another method is the *in situ* monitoring of the temperature of the IJJs so that self-heating can be detected and accordingly subtracted.^{18–21}

Self-heating can also be significantly reduced in small mesa structures, as is demonstrated in several theoretical discussions.^{13,15,19} In general, the temperature rise is proportional to the power generated in the mesa, $\Delta T \propto P = IV$. Since the current I is proportional to the junction area S and the voltage V to the junction number N in the mesa, reduction of S and N will effectively lessen heating in the IJJ mesa.

In this work, we report on a systematic study of ITSs when the self-heating effect is dramatically reduced by using ultra small mesas with S down to only $0.16 \mu\text{m}^2$. We will show that, starting from the IJJs with large S having considerable self-heating, the ITS undergoes significant change as S decreases down to the submicrometer level when heating is substantially reduced. This results in uniform ITSs which almost do not depend on the mesa size, at least up to voltages corresponding to the major conductance peaks, or somewhat higher. A brief comparison of our data to the STS and break-junction results will be presented.

II. EXPERIMENT

Our IJJs were fabricated on near optimally doped $\text{Bi}_2\text{Sr}_2\text{CaCu}_2\text{O}_{8+\delta}$ (Bi-2212) single crystals grown by the traveling solvent floating zone method. In our experiment, care has been taken to avoid the deterioration of the superconducting properties of the topmost surface CuO_2 double layers in the mesa during preparation so that all the layers in the mesa can be as identical as possible. This was realized through the *in situ* low-temperature cleavage of the crystals, immediately followed by evaporation of Au films at high speed.^{22,23} One major change to our previous work was that polymethylmethacrylate (PMMA) resist was used and mesa structures with lateral dimensions from 3.5 down to $0.4 \mu\text{m}$ were fabricated by electron beam lithography and Ar-ion milling. In the latter process, samples were also kept at liquid-nitrogen temperature to avoid possible oxygen loss in the mesa. Deposition and subsequent lift-off of a CaF_2 insulating layer were crucial in our experiment and could be successfully performed by careful resist treatment and thickness control of the CaF_2 layer.

The three-terminal configuration was used for the measurements of the resistance $R(T)$ and I - V curves in our experiments. The top Au film was used as both the current and voltage leads. $R(T)$ was measured using an ac excitation current ($1 \mu\text{A}$ for the largest mesas and 10 nA for the rest of the mesas) and lock-in amplifier. I - V curves were recorded using a dc method or by a digital oscilloscope with or without a preamplifier, and dI/dV curves were obtained by their numerical differentiation. Low-pass filters were used for all the leads and the measurements were performed in an electromagnetically shielded room.

III. SAMPLE CHARACTERIZATION

In Table I, we list the basic parameters of the two samples used in the present work. Samples *A* and *B* have four and five mesas respectively.²⁴ Symbols with and without a prime for the superconducting transition temperature and transition width correspond to the values of the surface and inner CuO_2

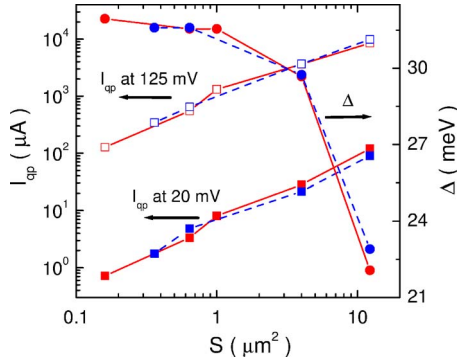


FIG. 1. (Color online) Junction-area dependence of the current at $V=20$ and 125 mV (left scale), and the energy gap Δ as determined from the conductance peak (right scale). The data are taken at $T_b=4.2$ K. The data with dashed and solid lines correspond to samples A and B, respectively.

double layers, which are obtained from the $R(T)$ measurements of the $12 \mu\text{m}^2$ IJJs. In Fig. 1, we show the quasiparticle current I_{qp} taken at $V=20$ mV (subgap) and 125 mV (above gap) from the I - V curves as a function of the nominal area S (V will be referred to as the measured values divided by N below). The data were taken at the bath temperature $T_b=4.2$ K. I_{qp} (or equivalently the mesa resistance) at both biases is seen to scale fairly well with S .

Low-voltage I - V curves of the largest ($12 \mu\text{m}^2$) and smallest ($0.36 \mu\text{m}^2$) mesas of sample A are shown in Fig. 2(a) and 2(b). The results were obtained without compensation for the resistance arising from the lead and contact of the surface layers with the electrode. From the figure, the branches can be clearly seen, indicating the IJJ number $N=10$ for the two mesas. The Josephson current ratio I'_c/I_c of the surface to inner IJJs is roughly 0.3 and 0.2 for the 12 and $0.36 \mu\text{m}^2$ mesas, respectively, which are consistent with our previous observations.^{22,23}

For the further analysis of the ITS data, two possible adverse effects need to be examined as the mesa area decreases. One is the influence of the contact resistance between the surface layers and the electrode. The other is the possible doping level change of the CuO_2 double layers in the mesa introduced during sample fabrication. In Fig. 2(c), we show the I - V characteristic of the surface IJJ for the $0.36 \mu\text{m}^2$ mesa measured using a scanning current of $\sim 0.5 \mu\text{A}$ and a preamplifier in the voltage channel. The result shows a basically vertical zero-bias critical current, which implies a negligible contact resistance compared with the mesa resistance.²⁵ In the worst case, if we estimate the contact resistance from the maximum possible slope change away from the ordinate, given by half the line width of about $50 \mu\text{V}$ that arises from noise, it turns out to be 55Ω . The

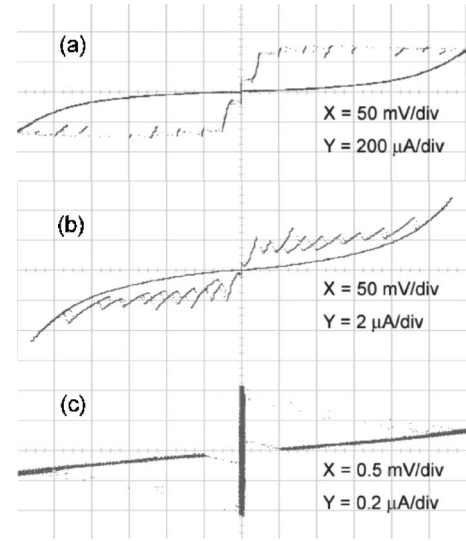


FIG. 2. I - V curve branches of the 12 (a) and $0.36 \mu\text{m}^2$ (b) mesa of sample A at $T_b=4.2$ K. (c) shows the surface IJJ's characteristic of the $0.36 \mu\text{m}^2$ mesa. Note the difference in the current and voltage scales.

real value is expected to be smaller due to the actual smaller slope change. If we use our previous data²³ of the specific resistance $\rho=1.5 \times 10^{-8} \Omega \text{cm}^2$, the contact resistance for the $0.36 \mu\text{m}^2$ mesa can be calculated to be 4.2Ω . All these values are considerably smaller than the mesa resistance²⁶ in the order of $4 \text{ k}\Omega$.

Next, we examine the possible doping level change in the mesa introduced during sample fabrication. In Fig. 3, we show the $R(T)$ characteristics of the four mesas of sample A. The scale is set for the $0.36 \mu\text{m}^2$ mesa and the R values for the larger mesas are multiplied by their area ratios relative to it. It can be seen that the $R(T)$ curve of the $12 \mu\text{m}^2$ mesa shows two clear superconducting transitions at $T_c=89$ K and $T'_c=71$ K, which correspond to the values of the inner and surface CuO_2 double layers, respectively. For the smaller mesas, the two transitions become successively broadened and shift toward lower temperatures. Nonetheless, we do not expect a significant doping level change as the mesa area decreases from the following considerations.

Franz *et al.* have investigated the properties of ultrasmall IJJs.²⁷ Their results show that there is a crossover temperature T^* , defined by $E_J(T^*)=kT^*$ where $E_J(T)=\hbar I_c(T)/2e$ is the Josephson coupling energy, above which no real Josephson current exists. This translates into a nonzero R in Fig. 3 for smaller mesas at temperatures near T_c and T'_c . From Fig. 2(b), for example, I_c at 4.2 K for the $0.36 \mu\text{m}^2$ mesa is $\sim 2.5 \mu\text{A}$ which corresponds to a Josephson energy $E_J \sim 60$ K. Considering the temperature dependence of E_J , I_c should vanish above a temperature somewhere below 60 K.²⁷ Similar consideration of I'_c of the surface junction in Fig. 2(c) leads to a temperature scale of 10 K. Hence, clear superconducting transitions at both T_c and T'_c should not be expected in the $R(T)$ characteristics for the small mesas.

The data in Fig. 3 show that for the four mesas, R rises with decreasing T toward T_c and their upturn slopes are not very different. This indicates that they have similar doping

TABLE I. Basic parameters of samples A and B.

Sample	T_c (K)	ΔT_c (K)	T'_c (K)	$\Delta T'_c$ (K)	N	S (μm^2)
A	89	0.9	71	2.3	10	12, 4, 0.64, 0.36
B	90	1.5	71.5	3.0	11	12, 4, 1, 0.64, 0.16

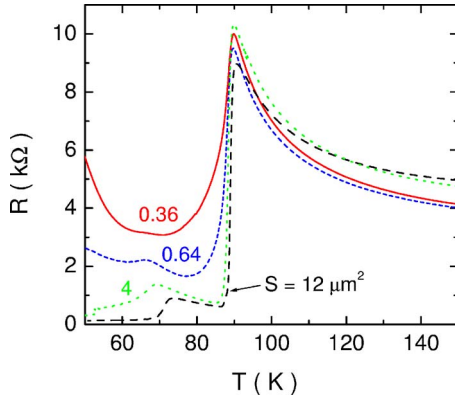


FIG. 3. (Color online) $R(T)$ characteristics of all mesas of sample A. R values are multiplied by the nominal area ratios relative to $S=0.36 \mu\text{m}^2$ for better comparison.

strength.²⁸ We also note that the starting point of the superconducting transition is nearly the same for these mesas. If we look at T_c (defined by the midpoint at the transition), we find that the value for the $0.64 \mu\text{m}^2$ mesa is only 1.3 K lower than that for the $12 \mu\text{m}^2$ mesa. For the $0.36 \mu\text{m}^2$ mesa, the broadening at the transition is larger due to the further decreasing I_c .

In Fig. 4, we show the dI/dV curves at $T_b=4.2$ K for the mesas with different area S in sample B. The curves show in general the well-known peak, dip, and hump, which all shift toward higher voltage as the area decreases. The peak is seen to become successively less sharp and its position, which corresponds to twice the superconducting energy gap Δ , has a sign of saturation with decreasing area. Δ versus S is plotted in Fig. 1 (right scale) for both samples A and B.

The energy gap Δ is found in many tunneling experiments^{2,9–12} to increase noticeably with decreasing doping. The saturation behavior in Figs. 1 and 4 therefore provides a clear evidence that the doping level change is not the major cause for the evolution of the dI/dV spectra as area decreases. This should particularly be the case considering that if the doping level change during sample fabrication were the cause for the spectra evolution in Figs. 1 and 4, its influence should be larger when the area gets smaller, due to the increase of the ratio of perimeter to area, and saturation should not result.

Below we will analyze the influence of the self-heating effect on the ITSS based on the model of Krasnov *et al.*¹⁹ It will be shown that for the smallest IJJ, the heating-induced temperature rise is around 5 K at the voltage bias corresponding to the superconducting peak. The spectra difference between the large and small mesas can then be explained in terms of the gradual decrease of Joule heating as the IJJ size decreases.

IV. INTRINSIC TUNNELING SPECTROSCOPY AND SELF-HEATING EFFECT

To get a quantitative picture of self-heating in IJJs, we consider a recent theory of Krasnov *et al.*¹⁹ According to this theory, the temperature rise for an IJJ mesa at given bias is

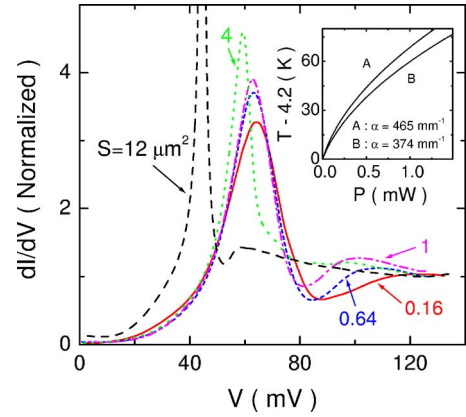


FIG. 4. (Color online) Normalized conductance of mesas with different area S in sample B measured at $T_b=4.2$ K. The inset shows the temperature rise against power for samples A and B as calculated from Eq. (2) with $T_b=4.2$ K.

governed by the ballistic phonon transport and can be estimated from

$$\Delta T \propto \frac{P}{\kappa_{ab} l_{ph}}, \quad (1)$$

where κ_{ab} and l_{ph} are the in-plane thermal conductivity and phonon mean free path, respectively. We note that κ_{ab} for the Bi-2212 materials has a strong temperature dependence in the range of 4.2–70 K and this should be taken into account in the estimation of ΔT .¹⁹ From the experimental data,²⁹ κ_{ab} can be well approximated by a linear temperature dependence as κ_{ab} (W/K m) $\approx 2.4 + 0.06T$ (K). Hence, neglecting the temperature dependence of l_{ph} , we can rewrite Eq. (1) as

$$T - T_b = \frac{\alpha P}{2.4 + 0.06T}, \quad (2)$$

where α is a constant to be determined. Equation (2) is a quadratic equation which can be solved directly. For $T_b = 4.2$ K, we have $T \approx \sqrt{488.4 + 16.7\alpha P} - 17.9$. To determine α , we consider the mesas with $S=12 \mu\text{m}^2$ at the bias corresponding to the sharp conductance peak. For sample B at this bias point, the power found from the $I-V$ curve is $P = 1.16$ mW, and the mesa temperature under heating is expected to be below T_c . In fact, $T \approx 70$ K can be estimated (see below in the case of sample A). Using these values, we find that $\alpha \approx 374 \text{ mm}^{-1}$. Similarly, we find³⁰ $P = 1.05$ mW and $T \approx 75$ K for sample A, and α is calculated to be 465 mm^{-1} . With these results, the temperature rise against P can be calculated, which is plotted in the inset of Fig. 4.

For the smallest mesa with $S=0.16 \mu\text{m}^2$ of sample B, we find that the temperature rise is 4.8 and 11 K at the voltages corresponding to the conductance peak and dip, respectively. For the mesa with $S=0.36 \mu\text{m}^2$ of sample A, the corresponding values are 12 and 29 K.

In Fig. 5, we show the temperature dependence of the $I-V$ (upper) and dI/dV (lower) curves of the mesa with $S=0.36 \mu\text{m}^2$ in sample A.³¹ The $I-V$ curves with symbols are from the mesa with $S=12 \mu\text{m}^2$ in the same sample for $T_b=4.2$ K (open squares) and 75 K (solid squares) respec-

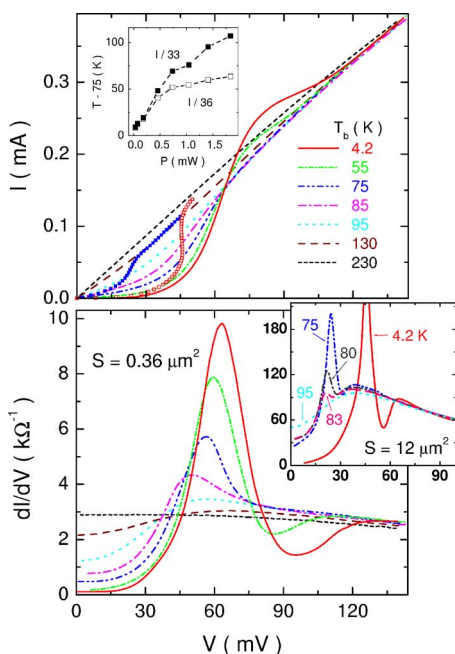


FIG. 5. (Color online) I - V (upper) and dI/dV (lower) curves at various temperatures for the mesa of $S=0.36 \mu\text{m}^2$ in sample A. The lower inset shows the dI/dV data of the mesa with $S=12 \mu\text{m}^2$ in the same sample. The I - V curves of this larger mesa at $T_b=4.2$ K (open squares) and 75 K (solid squares) are plotted in the upper panel with their current divided by the area ratio of the two mesas. The upper inset shows the temperature rise of the larger mesa at $T_b=75$ K against power as obtained directly from the comparison of the experimental I - V curves. See text for further details.

tively, which are plotted with their current scale reduced by the area ratio of the two mesas. The dI/dV curves of this larger mesa are shown in the lower inset for several temperatures.

Comparing the I - V curves in Fig. 5, we can see that the results of the larger mesa at 45 and 75 K both have steep current “jumps” that are quite common for quasiparticle tunneling characteristics. The current jump of the 4.2 K curve is primarily located across the corresponding regions of the smaller mesa at different temperatures, indicating that it reflects the superconducting gap but suffers from the gap reduction as a result of self-heating, which would lead to an unusually sharp peak in the dI/dV curve (see the lower inset). The current jump of the 75 K curve, on the other hand, is at a voltage well below the gap voltage of the smaller mesa. Turning to the temperature dependence of the dI/dV curves in the figure, we can see that the data for the two mesas are essentially different near T_c . While the small mesa shows a single conductance peak near T_c , the larger mesa still keeps the peak-dip-hump structure with its peak located at V considerably lower than the peak position of the small mesa.

The above analysis indicates that the temperature rise in the small mesa below the gap voltage is not severe³² and its temperature-dependent I - V curves can therefore be used to determine the temperature rise at each bias point in the I - V curves of the larger mesa (with I scaled according to the area ratio) if we assume that the two mesas are all the same ex-

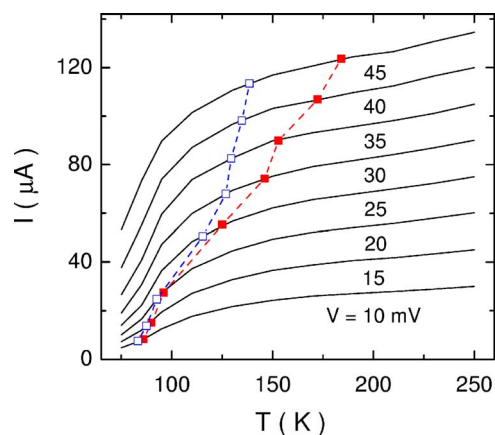


FIG. 6. (Color online) Current versus temperature at eight bias voltages as determined from the $0.36 \mu\text{m}^2$ mesa of sample A. Symbols correspond to the $12 \mu\text{m}^2$ mesa, with current divided by a factor of 33 (solid squares) or 36 (open squares) at the given bias voltages, from which the temperature rise at each point can be found.

cept for their area. In Fig. 6, we plot the temperature dependence of the current at several bias voltages for the small mesa. Solid squares are the current and voltage values taken from the I - V curve of the larger mesa at 75 K in Fig. 5, from which the heating-elevated temperature can be found. The temperature rise against power can also be obtained and is plotted in the upper inset of Fig. 5 (line with solid symbols). The T - P dependence resembles the calculated results shown in the inset of Fig. 4 although $\kappa_{ab}(T)$ is different for the temperatures below and above 70 K.²⁹ We point out that the result depends sensitively on the area ratio used. The data shown as a line with open symbols in the same inset are obtained for an area ratio of 36 (an area uncertainty below 10% is experimentally possible).

These results imply that if the temperature rise of the larger mesa at 75 K would follow the power dependence shown in the upper inset of Fig. 5, it will produce the measured I - V curve in the figure (solid squares). From this point of view, the conductance peak in the corresponding dI/dV curve should mainly result from self-heating and the gap feature in the curve is greatly distorted. This is understandable if we notice that, for a fixed V , the rate of the current increase with increasing temperature is different at different temperatures, which can be seen in Fig. 5. In particular, for $V \approx 25$ mV around which the conductance peak of the dI/dV curve at 75 K is located, the current rise between $T_b=75$ and 95 K contributes to more than a third of the total current rise from $T_b=4.2$ to 250 K. As a result, with relatively uniform rise of the temperature shown in the upper inset of Fig. 5, the current rise is much faster around the temperature range of 75–95 K, which leads to the peak in the dI/dV characteristics.

The tunneling spectra shown in the lower panel of Fig. 5 are qualitatively similar to the results of the STS and break-junction experiments. All the spectra demonstrate a typical dip-hump structure, which gradually vanishes as temperature increases. However, the temperature dependence of the spectra is somewhat different. In the present spectra, the peak

voltage in the dI/dV curves decreases and starts increasing again as the temperature rises across T_c , whereas the STS results generally show a weaker temperature dependence.⁹ Moreover, a closing gap near T_c is found in the break-junction experiments for optimally doped samples.¹¹ We note that the behavior similar to the present case has also been reported in ITS experiments using short-pulse measurement,² or submicrometer-sized IJJs made of Bi-2212 crystal whiskers,³ or intercalated samples that greatly reduce self-heating also for larger mesas.⁴

The spectral dip feature has been attributed to the coupling of bosonic excitations (either phonons or spin fluctuations) to the electronic system.^{12,33} In these explanations, the dip is located at an energy of $2\Delta + \Omega$, where Ω roughly corresponds to the energy of the bosonic excitations. In our case, we have $\Omega \approx 23$ and 25 meV for samples *A* and *B*, which are lower than in previous reports.^{12,33} Self-heating can be the cause for such a discrepancy since the temperature rise is still over 10 K at the bias near the dip, and the dip energy keeps on increasing in the case of the smallest mesas (see Fig. 4). The overall spectra therefore need more study using mesas with further reduced heating and crystals of different doping levels.

V. CONCLUSION

Mesa-structured IJJs on Bi-2212 crystals with areas ranging from 12 down to $0.16 \mu\text{m}^2$ have been successfully fabricated using electron beam lithography. It is demonstrated that self-heating decreases systematically with the reduction of junction area. For large-area junctions, self-heating can result in unusually sharp conductance peaks at low temperatures and also significantly distorted ITSs near T_c . In the case of the smallest junctions, a temperature rise of ~ 5 K at the bias corresponding to the conductance peak is estimated. The ITSs of these junctions show the well-known peak-dip-hump structure and a distinctive temperature dependence which deserves further study.

ACKNOWLEDGMENTS

We are grateful to H. B. Wang for kindly providing us with the Bi-2212 crystals, and to Y. F. Ren and H. W. Yu for their assistance during sample preparation. This work was supported by the Ministry of Science and Technology of China and by the National Center for Nanoscience and Technology of China.

*Electronic address: spzhao@aphy.iphy.ac.cn

- ¹V. M. Krasnov, A. Yurgens, D. Winkler, P. Delsing, and T. Claesson, *Phys. Rev. Lett.* **84**, 5860 (2000); V. M. Krasnov, A. E. Kovalev, A. Yurgens, and D. Winkler, *ibid.* **86**, 2657 (2001).
- ²M. Suzuki, T. Watanabe, and A. Matsuda, *Phys. Rev. Lett.* **82**, 5361 (1999); M. Suzuki and T. Watanabe, *ibid.* **85**, 4787 (2000).
- ³Yu. I. Latyshev, S. J. Kim, V. N. Pavlenko, T. Yamashita, and L. N. Bulaevskii, *Physica C* **362**, 156 (2001).
- ⁴A. Yurgens, D. Winkler, T. Claesson, S. J. Hwang, and J. H. Choy, *Int. J. Mod. Phys. B* **13**, 3758 (1999).
- ⁵A. Yurgens, D. Winkler, T. Claesson, S. Ono, and Yoichi Ando, *Phys. Rev. Lett.* **90**, 147005 (2003).
- ⁶Y. Yamada, K. Anagawa, T. Shibauchi, T. Fujii, T. Watanabe, A. Matsuda, and M. Suzuki, *Phys. Rev. B* **68**, 054533 (2003).
- ⁷R. Kleiner, F. Steinmeyer, G. Kunkel, and P. Müller, *Phys. Rev. Lett.* **68**, 2394 (1992); R. Kleiner and P. Müller, *Phys. Rev. B* **49**, 1327 (1994).
- ⁸For a review, see A. Yurgens, *Supercond. Sci. Technol.* **13**, R85 (2000).
- ⁹C. Renner, B. Revaz, J. Y. Genoud, K. Kadowaki, and Ø. Fischer, *Phys. Rev. Lett.* **80**, 149 (1998); C. Renner, B. Revaz, K. Kadowaki, I. Maggio-Aprile, and Ø. Fischer, *ibid.* **80**, 3606 (1998).
- ¹⁰M. Kugler, Ø. Fischer, C. Renner, S. Ono, and Y. Ando, *Phys. Rev. Lett.* **86**, 4911 (2001).
- ¹¹N. Miyakawa, P. Guptasarma, J. F. Zasadzinski, D. G. Hinks, and K. E. Gray, *Phys. Rev. Lett.* **80**, 157 (1998); N. Miyakawa, J. F. Zasadzinski, L. Ozyuzer, P. Guptasarma, D. G. Hinks, C. Kendziora, and K. E. Gray, *ibid.* **83**, 1018 (1999).
- ¹²J. F. Zasadzinski, L. Ozyuzer, N. Miyakawa, K. E. Gray, D. G. Hinks, and C. Kendziora, *Phys. Rev. Lett.* **87**, 067005 (2001).
- ¹³V. M. Krasnov, A. Yurgens, D. Winkler, and P. Delsing, *J. Appl. Phys.* **89**, 5578 (2001).

- ¹⁴J. C. Fenton, P. J. Thomas, G. Yang, and C. E. Gough, *Appl. Phys. Lett.* **80**, 2535 (2002).
- ¹⁵J. C. Fenton and C. E. Gough, *J. Appl. Phys.* **94**, 4665 (2003).
- ¹⁶K. Anagawa, Y. Yamada, T. Shibauchi, and M. Suzuki, *Appl. Phys. Lett.* **83**, 2381 (2003).
- ¹⁷V. N. Zavaritsky, *Phys. Rev. Lett.* **92**, 259701 (2004).
- ¹⁸A. Yurgens, D. Winkler, T. Claesson, S. Ono, and Y. Ando, *Phys. Rev. Lett.* **92**, 259702 (2004).
- ¹⁹V. M. Krasnov, M. Sandberg, and I. Zogaj, *Phys. Rev. Lett.* **94**, 077003 (2005).
- ²⁰H. B. Wang, T. Hatano, T. Yamashita, P. H. Wu, and P. Müller, *Appl. Phys. Lett.* **86**, 023504 (2005).
- ²¹M. H. Bae, J. H. Choi, and H. J. Lee, *Appl. Phys. Lett.* **86**, 232502 (2005).
- ²²X. B. Zhu, S. P. Zhao, G. H. Chen, H. J. Tao, C. T. Lin, S. S. Xie, and Q. S. Yang, *Physica C* **403**, 52 (2004).
- ²³S. P. Zhao, X. B. Zhu, Y. F. Wei, G. H. Chen, Q. S. Yang, and C. T. Lin, *Phys. Rev. B* **72**, 184511 (2005).
- ²⁴In our experiment, six mesas with sizes of 3.5 , 2 , 1 , 0.8 , 0.6 , and $0.4 \mu\text{m}$ were designed on each crystal. However, usually three to five mesas finally turned out to be successful. Here samples *A* and *B* are chosen out of about 16 samples we fabricated.
- ²⁵The lead resistance is roughly 1Ω , which can be neglected in the present case.
- ²⁶We use the value at 150 K (see Fig. 3). This value is slightly higher than the junction's normal-state resistance ($\sim 3.65 \text{ k}\Omega$) but lower than the resistance at the gap voltage at 4.2 K ($\sim 4.47 \text{ k}\Omega$).
- ²⁷A. Franz, Y. Koval, D. Vasyukov, P. Müller, H. Schneidewind, D. A. Ryndyk, J. Keller, and C. Helm, *Phys. Rev. B* **69**, 014506 (2004).
- ²⁸T. Watanabe, T. Fujii, and A. Matsuda, *Phys. Rev. Lett.* **79**, 2113

- (1997).
- ²⁹Y. Ando, J. Takeya, Y. Abe, K. Nakamura, and A. Kapitulnik, *Phys. Rev. B* **62**, 626 (2000).
- ³⁰Resistance of mesas with the same area but on separate crystals can be different, which results in different current and power for the same bias voltage. Since both T_c and T'_c from the $R(T)$ characteristics do not change, we believe that the resistance difference is a result of different stress upon the mesa introduced during sample fabrication.
- ³¹The smallest mesa with $S=0.16 \mu\text{m}^2$ in sample *B* was destroyed during its temperature dependence measurement.
- ³²We have shown a temperature rise of 12 K for this mesa at gap voltage and at $T_b=4.2$ K. Since κ_{ab} has a larger value at $T_b=75$ K, the temperature rise below the gap voltage is estimated to be less than 3.5 K.
- ³³J. F. Zasadzinski, L. Coffey, P. Romano, and Z. Yusof, *Phys. Rev. B* **68**, 180504(R) (2003).